Antagonist actions of CMK-1/CaMKI and TAX-6/Calcineurin along the *C. elegans* thermal avoidance circuit orchestrate nociceptive habituation

Martina Rudgalvyte[1], Zehan Hu[1], Dieter Kressler[1,2], Joern Dengjel[1], and Dominique A. Glauser[1,3]

[1], Department of Biology, University of Fribourg, 1700 Fribourg, Switzerland

[2], Metabolomics and Proteomics Platform (MAPP), Department of Biology, University of Fribourg, 1700 Fribourg, Switzerland

[3], Corresponding author dominique.glauser@unifr.ch

ABSTRACT

Habituation is a conserved physiological phenomenon, during which responses decrease following repeated exposure to innocuous or noxious stimuli. Impaired nociceptive habituation is associated with several pain conditions in human, but the underpinning molecular mechanisms are only partially understood. In the nematode *Caenorhabditis elegans*, thermo-nociceptive habituation was previously shown to be regulated by the Ca^{2+}/Calmodulin-dependent protein kinase 1 (named CMK-1), but its downstream effectors were unknown. Here, using *in vitro* kinase assays coupled with mass-spectrometry-based phosphoproteomics, we empirically identified hundreds of CMK-1 phospho-substrates. Among them, we found that CMK-1 can phosphorylate the calcineurin A (CnA) protein TAX-6 in a highly conserved regulatory domain. Combined genetic and pharmacological manipulations revealed a network of antagonistic actions between CMK-1 and calcineurin pathways in the regulation of the responsiveness of naïve worms and their habituation to repeated noxious heat stimuli. We further highlighted multiple places of action of the two signaling pathways in a subset of thermosensory neurons and downstream interneurons mediating avoidance behaviors. As a whole, our study has identified (i) CMK-1 substrate candidates, which will fuel further research on the intracellular actuation of CMK-1-dependent signaling, and (ii) a complex set of antagonistic interactions between CMK-1 and calcineurin signaling operating at distributed loci within a sensory-behavior circuit, acting to adjust baseline thermo-nociception and regulate thermo-nociceptive habituation.

INTRODUCTION

Animals from invertebrates to mammals can detect and avoid harmful stimuli, which is essential for their survival and well-being. Noxious stimuli are detected and encoded by specialized primary sensory neurons in a process called nociception (Dubin and Patapoutian 2010). Nociceptive signals are relayed in the nervous system via synaptic connections to be further processed and trigger different responses, such as behavioral changes and the perception of pain (Treede 1995). Pain sensitivity is not fixed and can be adjusted in various physiological and pathological contexts through nociceptive plasticity processes such as hyperalgesia or nociceptive desensitization/habituation (Kidd and Urban 2001, Sandkühler 2009, Rodriguez-Raecke, Doganci et al. 2010, Breimhorst, Hondrich et al. 2012, May, Rodriguez-Raecke et al. 2012, O'Neill, Brock et al. 2012, Basith, Cui et al. 2016). Prolonged or repeated exposure to noxious stimuli can lead to either sensitization or desensitization/habituation depending on the stimuli intensity, frequency and various physiological factors (Treede 1995). Because impaired nociceptive habituation is linked to various human chronic pain conditions (de Tommaso, Lo Sito et al. 2005, Smith, Tooley et al. 2008, de Tommaso, Federici et al. 2011), obtaining a deeper understanding of the cellular and molecular processes into play appears highly relevant to aid in the development of new therapeutical strategies for pain management. Several molecular mechanisms have been shown to modulate nociceptive pathways from the periphery to the brain (Kuner and Flor 2017, Pace, Passavanti et al. 2018, Amna, Salman et al. 2019), which involve the regulated activity of proteins such as membrane receptors or ion channels (involved in sensory-transduction, cell excitability, or signal conduction). Many kinases and phosphatases, which actuate protein regulation via the control of their phosphorylation status and that were previously shown to broadly regulate neural plasticity in the nervous system, are also involved in nociceptive plasticity (Willis Jr. 2001, Fu, Han et al. 2008, Wang and Zhang 2012, Isensee, Diskar et al. 2014, Pace, Passavanti et al. 2018). These regulatory pathways include intracellular signaling by calcium/calmodulin-dependent protein kinases (CaMKs) (Shum, Ko et al. 2005, Liang, Liu et al. 2012, Schild, Zbinden et al. 2014, Zhou, Liu et al. 2017), which might couple cellular activity levels with pleiotropic intracellular effects via post-translational modifications over a large repertoire of potential target proteins. Identifying the phosphorylation substrates of these kinases that act in the nociceptive pathway to mediate plasticity effects could provide relevant insight for future pain management translational research.

The nematode *Caenorhabditis elegans* has emerged as a powerful model to study the molecular and cellular bases of nociception and its plasticity. *C. elegans* produces innate avoidance behaviors in response to a variety of noxious stimuli, including irritant chemicals, harsh touch and noxious heat (Kaplan and Horvitz 1993, Wittenburg and Baumeister 1999, Hilliard, Apicella et al. 2005, Li, Kang et al. 2011, Liu, Schulze et al. 2012). Noxious heat stimuli targeting the animal head or the entire animal trigger a stereotyped reversal behavior (Wittenburg and Baumeister 1999, Liu, Schulze et al. 2012, Byrne Rodgers and Ryu 2020, Lia and Glauser 2020), which involves several thermo-sensory neurons, including AFD, AWC, and FLP, proposed to work as thermo-nociceptors (Chatzigeorgiou and Schafer 2011, Liu, Schulze et al. 2012, Kotera, Tran et al. 2016). The molecular components underpinning the function of the nociceptive system are well-conserved.

E.g., transient receptor potential (TRP) channels mediate worm thermo-nociceptive responses, like in fly and mammals (Chatzigeorgiou, Yoo et al. 2010, Glauser, Chen et al. 2011, Liu, Schulze et al. 2012, Nkambeu, Salem et al. 2020). Furthermore, persistent or repeated noxious heat stimuli cause a progressive reduction in the rate of heat-evoked reversals (Lia and Glauser 2020, Jordan and Glauser 2023), which we will refer to here as thermo-nociceptive habituation. A genetic screen for human pain-associated gene orthologs revealed thermo-nociceptive habituation alterations for many corresponding worm mutants, substantiating the interest of the model (Jordan and Glauser 2023). Among conserved molecular players, the worm CaMKI (named CMK-1) was shown to mediate thermo-nociceptive habituation (Schild, Zbinden et al. 2014, Lia and Glauser 2020, Jordan and Glauser 2023). CMK-1 is broadly expressed in the worm nervous system and, beyond thermo-nociceptive habituation, controls multiple experience-dependent plasticity processes, such as those related to developmental trajectories (Neal, Takeishi et al. 2015), the encoding of preferred growth temperature (Yu, Bell et al. 2014), salt aversive learning (Lim, Fehlauer et al. 2018) and habituation to repeated touch stimuli (Ardiel, McDiarmid et al. 2018). CMK-1 was shown to regulate the expression of the *guanylyl cyclase-8* (*gcy-8*) gene (Satterlee, Ryu et al. 2004), the AMPA glutamate receptor-1 (*glr-1)* gene (Moss, Park et al. 2016), the ortholog of the human DACH1/2 Dachsund transcription factor gene *(dac-1)* and the PY domain transmembrane protein-1 (*pyt-1*) gene (Harris, Bates et al. 2023). The impact of CMK-1 on gene transcription is partially mediated by the CREB homolog-1 (CRH-1) transcription factor (Harris, Bates et al. 2023), which could be phosphorylated by CMK-1 *in vitro* (Kimura, Corcoran et al. 2002) and in an heterologous expression system (Eto, Takahashi et al. 1999). A previous study used an *in silico* approach to systematically predict potential CMK-1 phosphorylation substrates and revealed repeated-touch habituation phenotypes in mutants for several candidate targets (Ardiel, McDiarmid et al. 2018). Apart from these few studies, we still know very little on the CMK-1 downstream effectors that mediate the numerous biological actions of CMK-1, including in mediating thermo-nociceptive habituation.

Calcineurin is a well-conserved eukaryotic Ca^{2+}/Calmodulin activated Serine/Threonine phosphatase (Klee, Crouch et al. 1979, Rusnak and Mertz 2000), involved in Ca^{2+} signaling pathway and functioning in several tissues, such as muscles, T cells and neurons, where it regulates synaptic plasticity and memory (Mukherjee and Soto 2011). Calcineurin regulates the activity of numerous proteins, such as transcription factors (Molkentin 2004), receptors, mitochondria proteins and microtubules depending on Ca^{2+} signaling state (Peuker, Strigli et al. 2022). Overexpression of calcineurin can cause cardiac hypertrophy (Gillis, Kavanagh et al. 2004, Yuan, Shen et al. 2024), higher infarct volumes (Dai, Hu et al. 2024), whereas lack of function can cause defects in kidney development (Gooch, Toro et al. 2004), and increase in autophagy (Ke, Huang et al. 2023). Chronic inhibition of calcineurin with immunosuppressant drugs, like cyclosporin A, was shown to cause irreversible neuropathic pain in some patients, a phenomenon referred to as calcineurin inhibitor-induced pain syndrome (Smith 2009). Several studies in mice have highlighted that calcineurin signaling modulate thermal nociception (Sato, Onaka et al. 2007). Several pathways working downstream of calcineurin signaling have been proposed to mediate the regulation of nociception, including NFAT transcription factors, TWIK-related spinal cord potassium channels (TRESK), TRP channels, and α2δ-1 Ca^{2+} channels (Smith 2009, Huang,

Chen et al. 2020, Huang, Chen et al. 2022). Nevertheless, we still have a cursory understanding of how calcineurin signaling integrates with other intracellular signaling pathways at different locus in the nociceptive circuit to orchestrate nociceptive plasticity.

Calcineurin is a heterodimeric protein consisting of one calcineurin A (CnA) catalytic subunit, and one calcineurin B (CnB) regulatory subunit. CnA contains catalytic and autoinhibitory domains, as well as CnB and Ca^{2+}/Calmodulin binding domains. In the absence of Ca^{2+} signaling, the autoinhibitory domain suppresses catalytic phosphatase activity. Increase in cytosolic Ca^{2+} promotes Ca^{2+} binding to CnB and to CaM. Ca^{2+}/CnB and Ca^{2+}/CaM in turn bind to calcineurin A subunit to release the autoinhibition, allow substrates to access the active site and thereby the activation of CnA (Bandyopadhyay, Lee et al. 2002, Kuhara, Inada et al. 2002, Wang, Du et al. 2008). *Caenorhabditis elegans* genome encodes one CnA homolog *tax-6 (*aka *cna-1)*, and one CnB homolog *cnb-1* displaying conserved structural and biochemical features with vertebrate calcineurin proteins (Bandyopadhyay, Lee et al. 2002, Bandyopadhyay, Lee et al. 2004). Lack of *tax-6* function causes thermal hypersensitivity and increased osmosensation, as well as increased adaptation of olfactory system (Kuhara, Inada et al. 2002). Loss-of-function mutants display a thermophilic behavior, and this anomaly could be rescued by wild type *tax-6* expression in AFD neurons. *tax-6* gain-of-function mutants show defective enteric muscle contraction (Lee, Song et al. 2005), as well as higher brood size and hypersensitivity to serotonin (Lee, Jee et al. 2004). The loss of *cnb-1* causes lethargic movements, delayed egg laying and reduced growth (Bandyopadhyay, Lee et al. 2002).

Here, we combined *in vitro* kinase assays with shotgun phosphoproteomics to empirically identify CMK-1 phospho-substrates in worm peptide and protein libraries. CMK-1 was found to phosphorylate CnA/TAX-6 in a highly conserved regulatory region, suggesting cross-regulation between CaMK and calcineurin signaling in worms. Follow-up genetic and pharmacological analyses confirmed a complex set of antagonistic signaling actions produced by the two pathways. However, the two intracellular signaling pathways appear to primarily function in separate neuron types to control thermo-nociceptive habituation. Collectively our results reveal multiple direct and indirect interactions between CaMK and calcineurin signaling and pave the role for deeper studies on the molecular control of nociceptive habituation in a simple genetic model.

RESULTS

CMK-1 phosphorylates multiple substrates *in vitro* including TAX-6/CnA

To identify phosphorylation substrates of CMK-1, we performed *in vitro* kinase assays on two types of substrate libraries followed by mass spectrometry-based phosphoproteomics (Fig. 1A). To that end, we purified recombinant CMK-1(1-295)T179D mutant protein produced in *E. coli*. This mutant is a constitutively active form of CMK-1 that lacks the C-terminal auto-inhibitory domain and harbors a T179D phosphomimic mutation, thus bypassing the need for Ca^{2+}/CaM binding and for phosphorylation by CKK-1. In two separate experiments, we assessed the phosphorylation produced by CMK-1(1-295)T179D, first, on a library of worm peptides produced by trypsin digestion of whole protein extracts and, second, on a whole protein library produced in non-denaturing conditions. As expected given the strong structural and functional conservation within the CaM kinase family, the consensus substrate motifs obtained with each substrate libraries matched the ΦXRXX(S/T)XXXΦ consensus previously characterized for mammalian CaMK (where Φ represents hydrophobic residues, Fig. 1B) (Lee, Kwon et al. 1994, White, Kwon et al. 1998). This result supports the validity of our *in vitro* kinase assays to identify direct CMK-1 targets and indicates that our experimental design efficiently mitigated the impact of any potential kinase activity coming from *E. coli* protein contamination or from worm kinases in the case of whole protein extracts.

With the peptide library data, we identified 646 phosphosites in 478 proteins (File S1). With the whole protein library, we identified 427 phosphosites in 365 proteins (File S1). Fifty-one phosphosites in 50 proteins were common between the two datasets (File S1, Fig.1B). As more extensively discussed later in the text (see Discussion section), these datasets are expected to include both phosphosites that are relevant CMK-1 target *in vivo* and 'false positive' phosphosites which are not relevant targets *in vivo*. These datasets are also expected to be biased toward abundant proteins, which are more likely to be detected. Consistent with this expectation, the most significant enrichment found via gene ontology (GO) term analyses in related to ribosomal and cytoskeletal proteins (File S2). Outside of these categories and among the phosphosites common to our two datasets, we were intrigued by the presence of a CMK-1 target phosphosite on the serine 443 of TAX-6/CnA. This phosphosite is located in a highly conserved region of TAX-6/CnA regulatory domain, just on the C-terminal side of the CaM binding domain (Fig. 1D). To confirm that CMK-1 can phosphorylate TAX-6/CnA S443 *in vitro*, we repeated the kinase assay using recombinant TAX-6/CnA protein purified from *E. coli* as substrate. Abundant phosphorylation of S443 was observed upon treatment with the constitutively active CMK-1 form, whereas this phosphorylation remained undetected with kinase-dead control treatment (Fig 1C). We conclude that CMK-1 can phosphorylate TAX-6/CnA on S443 *in vitro*.

Thermo-nociceptive habituation is impaired by CMK-1 down-regulation and by both up- and down-regulation of TAX-6/CnA

194 We previously reported that CMK-1 controls the habituation to persistent noxious heat
195 stimulations (Schild, Zbinden et al. 2014) or repeated stimulations (Lia and Glauser 2020). We
196 confirmed these previous observations by quantifying heat-evoked reversals in naïve animals
197 and animals submitted to a series repeated heat stimulation for one hour (habituation
198 treatment, Fig 2A). Whereas wild type response is significantly decreased following repeated
199 stimulation treatment (1h habituation), this habituation effect is almost absent in a *cmk-*
200 *1(ok287)* loss-of-function mutants (Fig. 2B). Conversely, a *cmk-1(syb1633)* gain-of-function
201 mutant with a CMK-1(T179D) over-activating mutation promoted a faster habituation (Fig. 2B and
202 Fig. 2-supplement 1). Therefore, our data confirm that CMK-1 activity is necessary and sufficient
203 to promote thermo-nociceptive habituation.

204 Since TAX-6/CnA is a CMK-1 kinase substrate *in vitro*, we hypothesized that it could take part in
205 the regulation of thermo-nociceptive habituation and evaluated the impact of genetic and
206 pharmacological manipulations down-regulating or up-regulating calcineurin signaling activity.
207 The permanent loss of TAX-6/CnA in *tax-6(p675)* mutants or of CnB/CNB-1 in a *cnb-1(jh103)* and
208 *cnb-1(ok276)* mutants caused a marked elevation in the rate of spontaneous reversals. While
209 this observation indicates that TAX-6/CnA signaling controls reversal behavior, the elevation was
210 so high that it precluded quantifying heat-evoked reversals and plasticity response. We next
211 turned to a pharmacological approach using the calcineurin inhibitor Cyclosporin A (Liu, Farmer
212 et al. 1991). Treating wild type worms with 10 mM Cyclosporin A for 24 h prior to behavioral
213 assays did not cause the problematic elevated spontaneous reversal phenotype, but
214 significantly reduced the thermal habituation effect (Fig.2C). An intact calcineurin signaling is
215 therefore required for thermo-nociceptive habituation. Next, we examined the impact of over-
216 activating TAX-6/CnA, using a *tax-6(jh107)* gain-of-function mutant lacking the auto-inhibitory C-
217 terminal domain of TAX-6/CnA, which we will refer to as *tax-6(gf)*. We noted a very slightly
218 enhanced reversal response in naïve *tax-6(gf)* mutants in comparison to wild type (Fig. 2D). More
219 strikingly, the habituation effect in *tax-6(gf)* mutants was strongly impaired. Therefore, our data
220 show that both overactivation and inhibition of TAX-6/CnA signaling can block thermo-
221 nociceptive habituation.

222 In summary, gain- and loss-of-function analyses highlight a CMK-1-dependent pathway
223 promoting and potentially two antagonistic TAX-6/CnA-dependent pathways that promote and
224 inhibit thermo-nociceptive habituation, respectively.

225 **CMK-1 and TAX-6/CnA signaling regulates thermo-nociceptive habituation through a set of**
226 **inhibitory cross-talks**

227 To assess the potential interactions between CMK-1 and calcineurin signaling in the control of
228 thermo-nociceptive habituation, we systematically tested combinations of up- or down-
229 regulating manipulations in the two pathways.

230 First, we examined the impact of down-regulating both CMK-1 and TAX-6/CnA signaling by
231 treating *cmk-1(lf)* mutants with Cyclosporin A. Surprisingly, whereas separate down-regulation
232 of either CMK-1 or TAX-6/CnA pathway strongly blocked habituation, their joint down-regulation
233 caused animals to habituate like wild type (Fig.3A). An intact habituation when both pathways
234 are inhibited supports the notion that CMK-1 and TAX-6/CnA represent regulators of one or more

habituation pathways that can also operate independently. In addition, this observation supports a model in which (i) the anti-habituation effect caused by CMK-1 inhibition is mediated by TAX-6/CnA and, conversely, (ii) that the anti-habituation effect caused by TAX-6/CnA inhibition requires intact CMK-1 activity.

Second, we tested the impact of simultaneously activating CMK-1 and calcineurin pathways by examining the behavior of *cmk-1(gf);tax-6(gf)* double mutants. We found that the double mutants behaved like *tax-6(gf)* single, entirely lacking habituation (Fig. 3B). Therefore, the pro-habituation effect of the CMK-1(T179D) activating mutation is fully blocked by TAX-6/CnA overactivation, which is compatible with a model in which CMK-1 over-activation might work by inhibiting calcineurin signaling.

Third, we assessed the impact of concomitantly up-regulating calcineurin and down-regulating CMK-1 signaling, by examining the behavior of *cmk-1(lf);tax-6(gf)* double mutants. Whereas the main phenotypic feature in each single mutant was a lack of habituation, the mutation combination produced a synthetic effect massively elevating spontaneous reversal, which precluded quantifying heat-evoked reversals.

Fourth, we tested the effect of concomitantly up-regulating CMK-1 activity and inhibiting calcineurin signaling by treating *cmk-1(gf)* mutants with Cyclosporin A. We found that, unlike in *cmk-1(wt)* background, Cyclosporin A treatment in *cmk-1(gf)* mutants did not prevent thermo-nociceptive habituation (Fig.3C). The fact that an overactive CMK-1 signaling can compensate for the inhibition of TAX-6/CnA suggests that the anti-habituation effect of calcineurin inhibition involves the ability to down-regulate CMK-1 signaling. Furthermore, the ability of CMK-1 overactivation to promote habituation when calcineurin is inhibited indicate that at least one CMK-1 regulatory branch works independently or downstream of calcineurin signaling.

Collectively, our results do not support a simple linear model in which CMK-1 would simply work upstream of TAX-6/CnA. Instead, our data suggest a model in which thermo-nociceptive habituation processed are regulated via the antagonist actions of CMK-1 and TAX-6/CnA signaling operating through a non-linear inhibitory network, such as the one depicted in Figure 3D and discussed below (see Discussion section).

CMK-1 acts in AFD and ASER sensory neurons to promote thermo-nociceptive habituation

Our next goal was to assess the place of action of CMK-1 signaling in the promotion of thermo-nociceptive habituation. To that end we used a neuron-specific rescue approach in the *cmk-1(lf)* background. We started our experiments by restoring CMK-1 expression in candidate thermo-sensory neurons, using *mec-3p* promoter to drive expression in FLP and *tax-4p* promoter to drive expression in AFD, AWC, ASI and ASE, as well as *glr-1p* promoter to drive expression in a subset of interneurons known to mediate reversal response. A positive control using *cmk-1p* promoter showed a partial, yet significant rescue effect (Fig. 4A). We observed a strong rescue effect with the *tax-4p* promoter, but no rescue effect with *mec-3p* or *glr-1p* (Fig. 4A). While not ruling out a contribution of other neurons, these data point to *tax-4*-expressing neurons as a major place of action for CMK-1 in the control of thermo-nociceptive habituation.

To further dissect the contribution of *tax-4*-expressing neurons, we conducted additional rescue experiments using *gpa-4p* to target ASI, a combination of *str-2p* and *srsx-3p* to target the two AWC neurons (AWCon and AWCoff, respectively), a combination of *gcy-5p* and *gcy-6p* to target ASEL and ASER neurons, *gcy-6* alone to target ASEL, *gcy-5p* alone to target ASER and *ttx-1p* to target AFD. We observed an almost total rescue effect with the *ttx-1p* promoter (AFD) and a more partial rescue effect with either *gcy-5p+gcy-6p* (both ASEL and ASER) or *gcy-5p* alone (only ASER) (Fig. 4B). No rescue effect was observed with the other promoters. We additionally tested the combined use of *ttx-1p* and *gcy-5p* to target both AFD and ASER and obtained a maximal rescue effect even stronger than with *ttx-1p* alone (Fig. 4B). Taken together, out data point to AFD as a major (and to ASER as a more minor) place of action for CMK-1 signaling in the control of thermo-nociceptive habituation to repeated heat-stimuli.

To further asses the role of AFD neurons, we evaluated the behavior of animals with genetically ablated AFD neurons. Interestingly, AFD neurons were dispensable for heat-evoked reversal responses in naïve animals under our experimental conditions, but required for the thermo-nociceptive habituation (Fig 4.C). We observed similar results when selectively inhibiting AFD neurotransmission in animals expressing the tetanus toxin (TeTx) in AFD (Fig. 4C).

Taken together, our results show that AFD neurons mediate thermo-nociceptive habituation and that intact CMK-1 signaling and neurotransmission in these neurons is essential for this process (Fig. 4D). ASER might represent an additional locus of CMK-1 action with a milder quantitative contribution to the process (Fig. 4D).

TAX-6/CnA activity in RIM and command interneurons inhibits thermo-nociceptive habituation

In order to assess the cellular place of action of TAX-6/CnA in the control of thermo-nociceptive habituation, we used a neuron-type-specific overactivation approach. We created transgenes containing a *tax-6(gf)* cDNA to drive the expression of the overactive, truncated form of TAX-6/CnA encoded in the *tax-6(jh107)* mutant. Like for CMK-1 rescue experiments above, we started by targeting candidate thermosensory neurons using either the *mec-3p* (FLP) or *tax-4p* (AFD, AWC, ASI and ASE) promoters, as well as interneurons with the *glr-1p* promoter. We examined the ability of the transgenes to replicate the two noticeable phenotypes of *tax-6(gf)* mutants: a slightly enhanced response in naïve animals and a strong impairment of habituation.

First, regarding naïve animal response, we found that *[mec-3p::tax-6(gf)]* and, to a lesser extent *[glr-1p::tax-6(gf)],* transgene caused a slight elevation in the heat-evoked response, whereas *[tax-4p:tax-6(gf)]* did not produce any effect (Fig. 5A). *glr-1p* promoter drives expression in several interneurons, including AVA, AVD, AVE and RIM whose activity is required and sufficient to trigger reversals (Alkema, Hunter-Ensor et al. 2005, Gray, Hill et al. 2005, Guo, Hart et al. 2009). To further dissect the specific interneurons involved, we expressed the *tax-6(gf)* transgene in AVA, AVD and AVE using the *nmr-1p* promoter, or the *lgc-39p* promoter, in RIM (and RIC) using the *cex-1p* promoter, and only in RIM using the *tdc-1p* promoter (Brockie, Mellem et al. 2001, Lemieux, Cunningham et al. 2015, Thapliyal, Beets et al. 2023). With all four promoters, we observed an

effect similar to that with *glr-1p*. Taken together, these results indicate that over-activating calcineurin signaling in *mec-3p*-expressing neuron (most likely in FLP thermo-nociceptor) or in a subset of reversal-mediating interneurons such as RIM or AVA/AVD/AVE is sufficient to up-regulate noxious heat-responsiveness in naïve animals (Fig 5C, top).

Second, regarding habituation to repeated heat stimuli, we found that the *[glr-1p::tax-6(gf)]* transgene could significantly reduce the habituation effect, leaving stronger response as compared to wild type after one hour of repeated stimulation (Fig. 5A). This effect was not as strong as the effect in *tax-6(gf)* mutant, which could be due to the transgene overexpression, mosaicism in the transgenic animals or to the fact that TAX-6/CnA overactivation in additional (unidentified) neurons could be also needed to reach the full effect. In contrast, the *[mec-3p::tax-6(gf)]* transgene did not affect nociceptive habituation, whereas the *[tax-4p::tax-6(gf)]* transgene produced a slight enhancement of habituation ($p<.05$). The data in Fig 5A suggest that one or more *glr-1*-expressing interneurons represent a major place of action in which overactive TAX-6/CnA signaling can act to inhibit habituation. We deepened the circuit analysis with additional promoters and observed a marked habituation defect caused with *cex-1p* and *tdc-1p* promoters, similar to that with *glr-1p* promoter, and a milder defect with *lgc-39p* and *nmr-1p* promoter. These results point to RIM second layer interneurons as primary locus and AVA/AVD/AVE reversal command neurons as secondary locus of overactive TAX-6/CnA action, while not ruling out the implication of additional neurons (Fig. 5C bottom).

DISCUSSION

CMK-1 substrate specificity is indistinguishable from that of mammalian CaMKs

Our knowledge on CaMK substrate specificity comes from numerous previous biochemical studies on mammalian CaMKs using synthetic peptide substrates at different scales (Lee, Kwon et al. 1994, White, Kwon et al. 1998, Corcoran, Joseph et al. 2003, Johnson, Yaron et al. 2023). Our study complements and extends this previous work through a large-scale identification of CaMKI substrates with endogenous peptide and protein libraries. With a dataset comprising several hundred substrates, we could confirm the ΦXRXX(S/T)XXXΦ consensus (where Φ represents hydrophobic residues) (Lee, Kwon et al. 1994, White, Kwon et al. 1998). These findings suggest that (i) the vast majority of our hits are direct CMK-1 substrates *in vitro* and (ii) the substrate specificity is conserved from worm to mammals.

Large-scale, empirically identification of CMK-1 phospho-targets

We have identified several hundred substrates that can be directly phosphorylated by CMK-1 *in vitro*. Our hit list is expected to include both substrates that are relevant *in vivo* and substrates that are not. Indeed, both the peptide library and the whole protein library datasets could include phosphosites coming from proteins that never encounter CMK-1 *in vivo*: e.g., non-neuronal proteins, secreted proteins, or proteins residing in specific organelles. In addition, the peptide library dataset could also include phosphosites in protein regions that are usually inaccessible to CMK-1 because of protein folding or protein complex formation. Furthermore, both datasets are expected to be biased toward abundant proteins, which are more likely to be detected. Accordingly, the strongest GO term enrichments in both datasets related to abundant and ubiquitous cellular components, involved in the translation process and cytoskeleton. Even if we cannot rule out an actual inclination of the CaM kinase pathway to regulate these processes, we suspect that these functional enrichments rather reflect an analytical bias. A previous study reported a list of 533 CMK-1 candidate substrates based on *in silico* predictions (Ardiel, McDiarmid et al. 2018). We found very little overlap between those predictions and our empirical datasets, with only 5 phosphosites shared with our peptide library list and 1 with our protein library list (Fig. 1-supplement 1). This limited overlap could be explained either by a limited exhaustiveness across the three datasets (high false negative rate) or come from limitations affecting *in silico* predictions. In support of the second explanation, we note that the previously predicted phosphosite list only very partially matches the empirically determined CMK-1 substrate consensus (Fig. 1-supplement 1). Because we lack a solid reference point, it is hard to estimate the false positive and false negative rates in our analyses at this stage. Additional experiments will be required to determine if the phosphorylation of these substrates is relevant *in vivo*, potentially on a case-by-case basis. Eventually, and keeping these limitations in mind, we believe that our large-scale dataset on the substrates which can by phosphorylated by CMK-1 *in vitro* will represent a useful resource in the search for CMK-1/CaMKI substrates mediating its numerous biological functions *in vivo*.

The phosphorylation of TAX-6/CnA by CMK-1/CaMKI

375 Previous *in vitro* studies have found that CnA can be phosphorylated by protein kinase C, casein
376 kinase I, casein kinase II, protein kinase C and by CaM kinase II (Hashimoto, King et al. 1988,
377 Hashimoto and Soderling 1989, Calalb, Kincaid et al. 1990, Rusnak and Mertz 2000). Here, we
378 show that *C. elegans* CaMKI CMK-1 can phosphorylate TAX-6/CnA on S443. This specific
379 phosphorylation event was confirmed in three different types of kinase assays: one using a
380 peptide library, one using a protein library, and one using purified recombinant TAX-6/CnA as
381 substrate. Ser 443 is located just downstream of the CaM binding domain in a highly conserved
382 region (Fig. 1D and E). This conserved serine was previously identified as a target of mammalian
383 CaMKII *in vitro* (Hashimoto, King et al. 1988, Hashimoto and Soderling 1989). Because TAX-
384 6/CnA and CMK-1 seem to mostly work from distinct neuronal cell-type to control nociceptive
385 habituation, it remains unclear whether TAX-6/CnA phosphorylation by CMK-1 is directly
386 relevant for the control of this process *in vivo*. Nevertheless, since the expression patterns of
387 CMK-1 and TAX-6/CnA largely overlap and since they are both activated by calcium signaling, we
388 speculate that this phosphorylation event might be relevant to other neuronal regulatory
389 signaling and we suggest it should be considered in future studies addressing the potential
390 cross-talks between the two pathways.

391 **Complex interaction network and distributed cellular locus of actions for CMK-1 and**
392 **Calcineurin signaling**

393 Our systematic analysis of CMK-1 and calcineurin signaling cross-talks has revealed a relatively
394 complex regulatory network in which the two pathways mostly antagonize each other to regulate
395 habituation. As mentioned above, habituation still takes place when CMK-1 and TAX-6/CnA are
396 concomitantly inhibited, which led us to model their action as regulatory events controlling a
397 separate habituation process (see model in Fig. 3D). While relatively complex, this model is the
398 simplest we could articulate to explain all the empirically measured interactions (see Fig.3-
399 supplement 1 for a case-by-case illustration of the proposed regulatory network functioning in
400 our different experimental conditions). In this model network, CMK-1 can regulate thermal
401 nociception via three pathways: in the first pathway CMK-1 promotes habituation by inhibiting
402 TAX-6/CnA, which in turn inhibits habituation. In the second and third pathways, CMK-1 works
403 independently of TAX-6/ CnA to inhibit and promote habituation, respectively. These two latter
404 pathways can each be gated by TAX-6/ CnA. Therefore, both CMK-1 and calcineurin signaling
405 activities may promote or inhibit habituation and shifting their activity balance could represent a
406 way to achieve nuanced yet robust modulation, integrating past activity with potentially
407 additional cues. This complex regulation scheme would be hard to achieve if the two signaling
408 pathways were working in a single neuronal cell type and it was therefore not surprising that our
409 cell-specific approaches revealed multiple cellular loci of action in the circuit controlling
410 temperature sensation and reversal execution.

411 In a previous study, CMK-1 was shown to work cell-autonomously in FLP to modulate thermo-
412 nociceptive responses following persistent noxious heat stimulation (Schild, Zbinden et al.
413 2014). FLPs are 'tonic' thermo-sensory neurons, whose activity constantly reflects the current
414 temperature (Saro, Lia et al. 2020). Here, we show that AFDs, but not FLPs, constitute the main
415 cellular locus of action of CMK-1-dependent plasticity in the case of repeated short-lasting
416 stimulations. Interestingly, AFD are mostly 'phasic' thermo-sensory neurons producing activity

417 peaks in response to thermal changes (Kimura, Miyawaki et al. 2004, Clark, Biron et al. 2006,
418 Hawk, Calvo et al. 2018, Glauser 2022). They are thus ideally suited to encode repeated thermal
419 pulses and modulate the heat-evoked reversal circuit. Laser-ablation of AFD was previously
420 shown to reduce reversal in response to head-targeted infra-red laser beams (Liu, Schulze et al.
421 2012). Here, we used thermal stimuli that were diffuse (whole animal exposure) and found that
422 neither the genetic ablation of AFD, nor the cell-specific inhibition of neurotransmission affected
423 the animal's ability to produce heat-evoked reversals. Instead, AFD was essential to favor an
424 experience-dependent reduction in heat-evoked reversal response. CMK-1 was previously
425 shown to mediate both short-term (minute timescale) and long-term (hour timescale)
426 adaptation in AFD intracellular calcium activity that resulted from thermal changes within the
427 15-25 °C innocuous temperature range (Yu, Bell et al. 2014). Long-term changes involved gene
428 expression changes, whereas the processes mediating short-term adaptation remained elusive
429 (Yu, Bell et al. 2014). At this stage, we do not know exactly how CMK-1 works in AFD to
430 orchestrate thermo-nociceptive habituation, but we can envision many possible mechanisms,
431 including qualitative or quantitative modulation of AFD thermo-sensitivity, neuronal excitability,
432 calcium dynamics, neurotransmitter or neuro-modulator release, or even developmental effect
433 affecting AFD synaptic connectivity. Additional studies will thus be needed to address the
434 downstream processes that are engaged within AFD to modulate animal responsiveness to
435 noxious heat stimuli.

436 We found that calcineurin signaling works at multiple cellular locus to control thermo-
437 nociceptive response. Overactive TAX-6 activity in FLP is sufficient to increase reversal response
438 in naïve animals. Since FLP activity is known to favor reversal response, we might hypothesize
439 that calcineurin activity could promote FLP activity. Overactive TAX-6 activity in RIM or, to a
440 lesser extent, in AVA/AVD/AVE neuron is sufficient to increase reversal response in naïve
441 animals, but conversely enhances reversal response upon repeated stimulation. This suggests
442 that the impact that calcineurin signaling has in these neurons depends on past experience.
443 AVA/AVD/AVE are thought to mostly promote reversal response, whereas RIM neuron activity
444 might either up-regulate, or down-regulate reversal responses based on the context (Alkema,
445 Hunter-Ensor et al. 2005, Gray, Hill et al. 2005, Guo, Hart et al. 2009, Piggott, Liu et al. 2011, Cho
446 and Sternberg 2014, Li, Zhou et al. 2023). Like for AFD above, multiple processes can potentially
447 be regulated by calcineurin to explain this complex regulation pattern, which will deserve further
448 attention.

449 **Conclusion**

450 In summary, we have revealed a complex signaling interplay between CMK-1 and calcineurin
451 signaling that operate via multiple regulatory nodes within the noxious-heat-evoked reversal
452 circuits of *C. elegans*. Together with the empirical identification of many additional potential
453 CMK-1 targets, our study paves the role for a deeper dissection of how conserved intracellular
454 signaling pathways operating at distributed loci within a sensory-behavior circuit can actuate
455 experience-dependent changes in nociceptive behavior.

456

457 **MATERIAL AND METHODS**

458 **Worm maintenance**

459 All *C. elegans* strains used in this study are listed in File S4. All strains were grown on nematode
460 growth media (NGM) plates with OP50 *E. coli* (Stiernagle, 2006) at 20°C. For TAX-6 inhibition
461 experiments, NGM plates containing cyclosporine A were used, as well as regular NGM plates as
462 control. Cyclosporine A (10 μM) plates were prepared 72h before experiments and kept protected
463 from light at room temperature.

464 **Expression and purification of CMK-1(T179D)-GST, CMK-1(K52A)-GST and TAX-6-HIS6**

465 DNA fragments encoding CMK-1 and TAX-6 proteins were PCR amplified and cloned into NdeI and
466 BamHI restriction sites of pDK2409 (pET-24d/GST-TEV-KAP104.419C) for the GST-TEV-tagged
467 protein and of pDK2832 (pET-24d/(His)6) for the His6-tagged proteins. Plasmids were transformed
468 into *E. coli* BL21 (DE3) (Novagen). For protein expression, bacteria were grown overnight at 37°C,
469 next day transferred to 200 ml of Luria Broth (LB) with kanamycin 30 μg/ml to OD_{600}=0.1, incubated
470 up to OD_{600}=0.5. Then, protein expression was induced using 0.5 mM isopropyl β-D-1-
471 thiogalactopyranoside (IPTG) and incubated for 5 h at 23 °C. After, bacteria cells were collected
472 by centrifugation at 2800 rcf for 10 min at 4°C, resuspended in cold lysis buffer (150 mM NaCl, 50
473 mM Tris-HCl pH7.5, 1.5 mM $MgCl_2$, 5% Glycerol, 1 mM phenylmethylsulfonyl fluoride (PMSF)) and
474 lysed in a Microfluidizer Processor M-110L. Then, NP-40 was added to the concentration of 0.1%,
475 and soluble extract was obtained by centrifugation at 23'400 rcf for 20 min at 4 °C. Supernatant
476 was incubated for 2 h at 4°C while rotating with Glutathione superflow beads (Qiagen) for GST-
477 tagged CMK-1 variants or nickel-nitrilotriacetic acid beads (Ni-NTA, Qiagen) in the presence of 15
478 mM imidazole for TAX-6-His6 protein binding. Beads were harvested at 580 rcf at 4 °C. GST-tagged
479 CMK-1 kinase was cleaved from the tag during incubation in lysis buffer (added 1 mM PMSF, 0.1%
480 NP-40, 1 mM Dithiothreitol (DTT)) with home-made TEV protease. TAX-6-bound Ni-NTA beads
481 were washed 7 times with imidazole-containing buffer (5x with 15 mM and 2x with 50 mM
482 imidazole) and eluted in lysis buffer with 1 mM PMSF, 0.1% NP-40, 500 mM imidazole. Protein
483 concentration was determined by Pierce Microplate BCA protein assay Kit-Reducing Agent
484 Compatible (Thermo Scientific) using BSA as protein standard.

485 **Total protein lysate preparation**

486 Worms were grown on 10 cm diameter plates to the stage of young adults, washed with distilled
487 water and suspended in extraction buffer. For *in vitro* kinase assays on peptide, urea buffer (8 M
488 urea, 50 mM Tris-HCl pH 8.5) was used. For *in vitro* kinase assays on intact proteins, native protein
489 extraction buffer (50 mM HEPES pH 7.4, 1% NP-40, 150 mM NaCl, 1x protease inhibitors, 0.5 mM
490 PMSF) was used. Worms were flash-frozen in liquid nitrogen and cryogenically disrupted by using
491 a Precellys homogenizer and acid-washed glass beads (5000 x 3 for 30 s with 30 s pause after
492 each cycle). Lysates were collected by centrifugation at 1500 rcf at 4 °C.

493 ***In vitro* kinase assay**

494 Purified CMK-1 kinase was used the same day to avoid freezing. *In vitro* kinase assays were
495 performed according to (Hu, Sankar et al. 2021). Briefly, for kinase assays performed on native
496 proteins, 30 mg of worm protein extract was incubated with pre-washed NHS-activated
497 Sepharose beads at 4°C on a rotor for 6 h. Beads were washed with 3 × 10 ml of phosphatase
498 buffer (50 mM HEPES, 100 mM NaCl, 0.1% NP-40). 1 ml of phosphatase buffer containing 5,000
499 to 10,000 units of lambda phosphatase with 1 mM $MnCl_2$ was added and incubated for 4 h at room

500 temperature (RT) followed by overnight incubation at 4°C on the rotor to dephosphorylate
501 endogenous proteins. Beads were washed with 2 × 10 ml of kinase buffer (50 mM Tris-HCl pH 7.6,
502 10 mM $MgCl_2$, 150 mM NaCl and 1x PhosSTOP (Roche)). Endogenous kinases bound to beads
503 were inhibited by incubation with 1 mM FSBA in 1 ml of kinase buffer at RT on the rotor for 2 h. In
504 addition, inhibition of the remaining active kinases was achieved with a further 1 h incubation in
505 the presence of staurosporine (LC Laboratories), added to a final concentration of 100 µM. The
506 beads were washed with 3 × 10 ml of kinase buffer to remove non-bound kinase inhibitors. The
507 supernatant was removed completely using gel loading tips. Beads were split into 6 tubes (3x with
508 kinase and 1 mM ATP, 3x with kinase and without ATP (Sigma-Aldrich), kinase buffer was added
509 and incubated for 4 h at 30°C while shaking. For TAX-6 phosphorylation by CMK-1 *in vitro* assay,
510 CMK-1 was kept on Glutathione superflow beads and purified TAX-6 protein in kinase buffer (50
511 mM HEPES pH7.5, 10 mM $Mg(Ac)_2$, 1 mM DTT, 1x PhosSTOP) was added onto protein/bead mix
512 together with ATP. Afterwards samples were lyophilized followed by protein digestion using
513 trypsin. Samples were chemically labeled using dimethyl-labeling (Boersema, Raijmakers et al.
514 2009) supporting relative MS-based quantification. For kinase assays performed on peptide
515 libraries, the procedure was the same except that protein extract samples were digested with Lyc-
516 C (Lysyl Endopeptidase, WAKO) for 4 h and trypsin (Promega) overnight, before incubating them
517 with Sepharose beads. Later beads were incubated either with purified active CMK-1 or kinase
518 dead CMK-1 in kinase buffer (50 mM Tris-HCl pH 7.6, 10 mM $MgCl_2$, 150 mM NaCl, 1x PhosSTOP,
519 1 mM DTT and 1 mM γ-[^{18}O4]-ATP (Cambridge Isotope Laboratories)).

520 Peptides were fractionated and phosphopeptides enriched as described (Hu, Sankar et al. 2021);
521 briefly: samples were incubated with TiO2 (GL Sciences) slurry, which was pre-incubated with 300
522 mg/ml lactic acid in 80% acetonitrile, 1% trifluoroacetic acid (TFA) prior to enrichment for 30 min
523 at RT. For elution, TiO2 beads were transferred to 200 µl pipette tips blocked by C8 discs. After
524 washing with 10% acetonitrile/1% TFA, 80% acetonitrile/1% TFA, and LC-MS grade water,
525 phosphopeptides were eluted with 1.25% ammonia in 20% acetonitrile and 1.25% ammonia in
526 80% acetonitrile. Eluates were acidified with formic acid, concentrated by vacuum concentration,
527 and resuspended in 0.1% formic acid for LC-MS/MS analysis.

528 ***LC-MS/MS analyses***

529 LC-MS/MS measurements were performed on two LC-MS/MS systems as described (Hu, Sankar
530 et al. 2021): a QExactive (QE) Plus and HF-X mass spectrometer coupled to an EasyLC 1000 and
531 EasyLC 1200 nanoflow-HPLC, respectively (all Thermo Scientific). Peptides were fractionated on
532 fused silica HPLC-column tips using a gradient of A (0.1% formic acid in water) and B (0.1% formic
533 acid in 80% acetonitrile in water): 5%–30% B within 85 min with a flow rate of 250 nl/min. Mass
534 spectrometers were operated in the data-dependent mode; after each MS scan (m/z = 370 – 1750;
535 resolution: 70'000 for QE Plus and 120'000 for HF-X) a maximum of ten, or twelve MS/MS scans
536 were performed (normalized collision energy of 25%), a target value of 1'000 (QE Plus)/5'000 (HF-
537 X) and a resolution of 17'500 for QE Plus and 30'000 for HF-X. MS raw files were analyzed using
538 MaxQuant (version 1.6.2.10) (Cox and Mann 2008) using a full-length *C. elegans* Uniprot database
539 (November, 2017), and common contaminants such as keratins and enzymes used for in-gel
540 digestion as reference. Carbamidomethylcysteine was set as fixed modification and protein
541 amino-terminal acetylation, serine-, threonine- and tyrosine- (heavy) phosphorylation, and
542 oxidation of methionine were set as variable modifications. In case of labeled samples, triple
543 dimethyl-labeling was chosen as quantification method (Boersema, Raijmakers et al. 2009). The
544 MS/MS tolerance was set to 20 ppm and three missed cleavages were allowed using trypsin/P as
545 enzyme specificity. Peptide, site, and protein FDR based on a forward-reverse database were set

546 to 0.01, minimum peptide length was set to 7, the minimum score for modified peptides was 40,
547 and minimum number of peptides for identification of proteins was set to one, which must be
548 unique. The "match-between-run" option was used with a time window of 0.7 min. MaxQuant
549 results were analyzed using Perseus (Tyanova, Temu et al. 2016).

550 **Worm preparation for heat avoidance assay and number of replicates**

551 Gravid adult worms were treated with hypochlorite solution according to standard protocol.
552 Embryos were rinsed twice with water and once with M9 buffer, then resuspended in M9 and
553 plated on NGM plates seeded with OP-50 *E. coli*. 200-300 embryos per individual plate were
554 seeded. Worms were incubated at 20°C until start of egg laying (65-90 h, depending on the strain
555 or condition). Worms were washed off the plates with distilled water, placed into 1.5 ml tubes and
556 washed twice more to remove bacterial residues. Worms were placed on unseeded NGM plates
557 and left to disperse and acclimate in the experimental room for 60 min. Prior to worm deposition,
558 these experimental unseeded plates were kept open in a laminar flow hood for 3 h to ensure dry
559 surface. Plate lid was removed 3 min before starting the assay. At least 3 replicates were
560 performed for each strain or condition on 3 separate days running wild-type N2 strain alongside.

561 For the experiments using transgenic animals, fluorescent signal-carrying worms were picked 16-
562 19 h before the experiment to allow for recovery.

563 **Heat stimulation and adaptation protocols**

564 INFERNO system (Lia and Glauser 2020) was used for heat stimulation and behavior recording.
565 The heat stimulation program is composed of a baseline period of 40 s without any heat
566 stimulation and 4 s with 400 W heating (4 IR lamps turned on). This program was applied at T0
567 (naïve animals) and T60 (adapted animals). For a duration of 1h worm plates were placed under
568 the ThermINATOR system providing infinitely looping temperature program composed of 4 s of IR
569 lamps stimulation, followed by 20 s ISI with the lamps turned off. In the INFERNO system, worm
570 plates were recorded using a DMK 33U×250 camera and movies acquired with the IC capture
571 software (The Imaging Source), at 8 frames per second, at a 1600×1800 pixel resolution, and the
572 resulting .AVI file was encoded as Y800 8-bit monochrome. The Multi-Worm Tracker 1.3.0 (MWT)
573 (Swierczek, Giles et al. 2011) with previously described configuration settings (Lia and Glauser
574 2020) was used for movie analyses. A previously described Python script was use to flag the frame
575 of reversal occurrence (Lia and Glauser 2020). Each reported data point corresponds to the
576 results of one assay plate scoring at least 50 animals.

577 **Transgene construction and transgenesis**

578 Promoter-containing Entry plasmids (Multi-site Gateway slot 1) were constructed by PCR using
579 N2 genomic DNA as template and primers flanked by attB4 and attB1r recombination sites; the
580 PCR product being cloned into pDONR-P4-P1R vector (Invitrogen) by BP recombination.

581 Coding sequence-containing Entry plasmids (Multi-site Gateway slot 2) were constructed by PCR
582 using N2 cDNA as template and primers flanked by attB1 and attB2 recombination sites; the PCR
583 product being cloned into pDONR_221 vector (Invitrogen) by BP recombination.

584 Expression plasmids for transgenesis were created through a LR recombination reaction
585 (Gateway™ LR Clonase, Invitrogen) as per the manufacturer's instructions.

586 Primer sequences for BP reactions and all plasmids used in this study are listed in File S4.

587 DNA constructs were transformed into competent DH5a *E. coli* (NEB C2987H), purified with the
588 GenElute HP Plasmid miniprep kit (Sigma) and microinjected in the worm gonad according to a
589 standard protocol (Evans 2006) together with co-injection markers for transgenic animal
590 identification. The concentrations of expression plasmids and co-markers injected are indicated
591 in File S4.

592 **Site-directed mutagenesis**

593 To create truncated *tax-6(gf)* transgene PCR-based site-directed mutagenesis (Hemsley, Arnheim
594 et al. 1989) was used. Entry plasmid containing *tax-6* coding DNA sequence was amplified with
595 the KOD Hot Start DNA Polymerase (Novagen; Merck). Primers were designed to contain the
596 desired deletion and phosphorylated in 5' end (File S4). Linear PCR products were purified from
597 agarose gel (1%) after electrophoresis with a Zymoclean-Gel DNA Recovery kit (Zymo Research),
598 circularized using DNA Ligation Kit <Mighty Mix> (Takara).

599 **Statistical analyses**

600 ANOVAs were conducted using Jamovi (The jamovi project (2022), jamovi (Version 2.3) [Computer
601 Software]; retrieved from (https://www.jamovi.org). Post hoc tests were used to compare each of
602 the mutants with wild type (N2) or *cmk-1(lf)* using Bonferroni–Holm correction.

603

604 **DATA AVAILABILITY**

605 MS data have been deposited to the ProteomeXchange Consortium via the PRIDE partner
606 repository with the dataset identifier PXD055776 (Perez-Riverol, Bai et al. 2022). The raw data and
607 *p* values presented in the different figures are provided in File S3.

608

609 **ACKNOWLEDGEMENTS**

610 We are grateful to Lisa Schild, Laurence Bulliard and Michael Stumpe for expert technical
611 support. Some strains were provided by the CGC, which is funded by NIH Office of Research
612 Infrastructure Programs (P40 OD010440). The study was supported by the Swiss National
613 Science Foundation (BSSGI0_155764, PP00P3_150681, and 310030_197607 to DAG,
614 310030_212187 to JD) and by the Novartis Foundation for Medical-Biological Research.

615

616 **COMPETING INTERESTS**

617 No competing interests declared

618

619

620

621

622

REFERENCES

Alkema, M. J., M. Hunter-Ensor, N. Ringstad and H. R. Horvitz (2005). "Tyramine Functions independently of octopamine in the Caenorhabditis elegans nervous system." Neuron **46**(2): 247-260.

Amna, K., K. Salman and K. Yeong Shik (2019). "Insight into Pain Modulation: Nociceptors Sensitization and Therapeutic Targets." Current Drug Targets **20**(7): 775-788.

Ardiel, E. L., T. A. McDiarmid, T. A. Timbers, K. C. Y. Lee, J. Safaei, S. L. Pelech and C. H. Rankin (2018). "Insights into the roles of CMK-1 and OGT-1 in interstimulus interval-dependent habituation in Caenorhabditis elegans." **285**(1891): 20182084.

Bandyopadhyay, J., J. Lee and A. Bandyopadhyay (2004). "Regulation of calcineurin, a calcium/calmodulin-dependent protein phosphatase, in C. elegans." Mol Cells **18**(1): 10-16.

Bandyopadhyay, J., J. Lee, J. Lee, J. I. Lee, J. R. Yu, C. Jee, J. H. Cho, S. Jung, M. H. Lee, S. Zannoni, A. Singson, D. H. Kim, H. S. Koo and J. Ahnn (2002). "Calcineurin, a calcium/calmodulin-dependent protein phosphatase, is involved in movement, fertility, egg laying, and growth in Caenorhabditis elegans." Mol Biol Cell **13**(9): 3281-3293.

Basith, S., M. Cui, S. Hong and S. Choi (2016). "Harnessing the Therapeutic Potential of Capsaicin and Its Analogues in Pain and Other Diseases." Molecules (Basel, Switzerland) **21**(8): 966.

Boersema, P. J., R. Raijmakers, S. Lemeer, S. Mohammed and A. J. Heck (2009). "Multiplex peptide stable isotope dimethyl labeling for quantitative proteomics." Nat Protoc **4**(4): 484-494.

Breimhorst, M., M. Hondrich, C. Rebhorn, A. May and F. Birklein (2012). "Sensory and sympathetic correlates of heat pain sensitization and habituation in men and women." Eur J Pain **16**(9): 1281-1292.

Brockie, P. J., J. E. Mellem, T. Hills, D. M. Madsen and A. V. Maricq (2001). "The C. elegans glutamate receptor subunit NMR-1 is required for slow NMDA-activated currents that regulate reversal frequency during locomotion." Neuron **31**(4): 617-630.

Byrne Rodgers, J. and W. S. Ryu (2020). "Targeted thermal stimulation and high-content phenotyping reveal that the C. elegans escape response integrates current behavioral state and past experience." PLOS ONE **15**(3): e0229399.

Calalb, M. B., R. L. Kincaid and T. R. Soderling (1990). "Phosphorylation of calcineurin: Effect on calmodulin binding." Biochemical and Biophysical Research Communications **172**(2): 551-556.

Chatzigeorgiou, M. and William R. Schafer (2011). "Lateral Facilitation between Primary Mechanosensory Neurons Controls Nose Touch Perception in C. elegans." Neuron **70**(2): 299-309.

Chatzigeorgiou, M., S. Yoo, J. D. Watson, W. H. Lee, W. C. Spencer, K. S. Kindt, S. W. Hwang, D. M. Miller, 3rd, M. Treinin, M. Driscoll and W. R. Schafer (2010). "Specific roles for DEG/ENaC and TRP channels in touch and thermosensation in C. elegans nociceptors." Nat Neurosci **13**(7): 861-868.

Cho, J. Y. and P. W. Sternberg (2014). "Multilevel modulation of a sensory motor circuit during C. elegans sleep and arousal." Cell **156**(1-2): 249-260.

Clark, D. A., D. Biron, P. Sengupta and A. D. Samuel (2006). "The AFD sensory neurons encode multiple functions underlying thermotactic behavior in Caenorhabditis elegans." J Neurosci **26**(28): 7444-7451.

Corcoran, E. E., J. D. Joseph, J. A. MacDonald, C. D. Kane, T. A. J. Haystead and A. R. Means (2003). "Proteomic Analysis of Calcium/Calmodulin-dependent Protein Kinase I and IV in Vitro Substrates Reveals Distinct Catalytic Preferences*." Journal of Biological Chemistry **278**(12): 10516-10522.

Cox, J. and M. Mann (2008). "MaxQuant enables high peptide identification rates, individualized p.p.b.-range mass accuracies and proteome-wide protein quantification." Nat Biotechnol **26**(12): 1367-1372.

Dai, F., C. Hu, X. Li, Z. Zhang, H. Wang, W. Zhou, J. Wang, Q. Geng, Y. Dong and C. Tang (2024). "Cav3.2 channel regulates cerebral ischemia/reperfusion injury: a promising target for intervention." Neural Regen Res **19**(11): 2480-2487.

de Tommaso, M., A. Federici, R. Santostasi, R. Calabrese, E. Vecchio, G. Lapadula, F. Iannone, P. Lamberti and P. Livrea (2011). "Laser-Evoked Potentials Habituation in Fibromyalgia." The Journal of Pain **12**(1): 116-124.

de Tommaso, M., L. Lo Sito, O. Di Fruscolo, M. Sardaro, M. Pia Prudenzano, P. Lamberti and P. Livrea (2005). "Lack of habituation of nociceptive evoked responses and pain sensitivity during migraine attack." Clin Neurophysiol **116**(6): 1254-1264.

Dubin, A. E. and A. Patapoutian (2010). "Nociceptors: the sensors of the pain pathway." J Clin Invest **120**(11): 3760-3772.

Eto, K., N. Takahashi, Y. Kimura, Y. Masuho, K. Arai, M. A. Muramatsu and H. Tokumitsu (1999). "Ca(2+)/Calmodulin-dependent protein kinase cascade in Caenorhabditis elegans. Implication in transcriptional activation." J Biol Chem **274**(32): 22556-22562.

Evans, T. C., (ed) (2006). "Transformation and microinjection." WormBook.

Fu, Y., J. Han, T. Ishola, M. Scerbo, H. Adwanikar, C. Ramsey and V. Neugebauer (2008). "PKA and ERK, but not PKC, in the amygdala contribute to pain-related synaptic plasticity and behavior." Mol Pain **4**: 26.

Gillis, A. M., K. M. Kavanagh, H. J. Mathison, J. R. Somers, S. Zhan and H. J. Duff (2004). "Heart block in mice overexpressing calcineurin but not NF-AT3." Cardiovasc Res **64**(3): 488-495.

Glauser, D. A. (2022). "Temperature sensing and context-dependent thermal behavior in nematodes." Curr Opin Neurobiol **73**: 102525.

Glauser, D. A., W. C. Chen, R. Agin, B. L. Macinnis, A. B. Hellman, P. A. Garrity, M. W. Tan and M. B. Goodman (2011). "Heat avoidance is regulated by transient receptor potential (TRP) channels and a neuropeptide signaling pathway in Caenorhabditis elegans." Genetics **188**(1): 91-103.

Gooch, J. L., J. J. Toro, R. L. Guler and J. L. Barnes (2004). "Calcineurin A-alpha but not A-beta is required for normal kidney development and function." Am J Pathol **165**(5): 1755-1765.

Gray, J. M., J. J. Hill and C. I. Bargmann (2005). "A circuit for navigation in Caenorhabditis elegans." Proc Natl Acad Sci U S A **102**(9): 3184-3191.

Guo, Z. V., A. C. Hart and S. Ramanathan (2009). "Optical interrogation of neural circuits in Caenorhabditis elegans." Nat Methods **6**(12): 891-896.

Harris, N., S. G. Bates, Z. Zhuang, M. Bernstein, J. M. Stonemetz, T. J. Hill, Y. V. Yu, J. A. Calarco and P. Sengupta (2023). "Molecular encoding of stimulus features in a single sensory neuron type enables neuronal and behavioral plasticity." Current Biology **33**(8): 1487-1501.e1487.

Hashimoto, Y., M. M. King and T. R. Soderling (1988). "Regulatory interactions of calmodulin-binding proteins: phosphorylation of calcineurin by autophosphorylated Ca2+/calmodulin-dependent protein kinase II." Proc Natl Acad Sci U S A **85**(18): 7001-7005.

Hashimoto, Y. and T. R. Soderling (1989). "Regulation of calcineurin by phosphorylation. Identification of the regulatory site phosphorylated by Ca2+/calmodulin-dependent protein kinase II and protein kinase C." J Biol Chem **264**(28): 16524-16529.

Hawk, J. D., A. C. Calvo, P. Liu, A. Almoril-Porras, A. Aljobeh, M. L. Torruella-Suarez, I. Ren, N. Cook, J. Greenwood, L. Luo, Z. W. Wang, A. D. T. Samuel and D. A. Colon-Ramos (2018). "Integration of Plasticity Mechanisms within a Single Sensory Neuron of C. elegans Actuates a Memory." Neuron **97**(2): 356-367.e354.

Hemsley, A., N. Arnheim, M. D. Toney, G. Cortopassi and D. J. Galas (1989). "A simple method for site-directed mutagenesis using the polymerase chain reaction." Nucleic acids research **17**(16): 6545-6551.

Hilliard, M. A., A. J. Apicella, R. Kerr, H. Suzuki, P. Bazzicalupo and W. R. Schafer (2005). "In vivo imaging of C. elegans ASH neurons: cellular response and adaptation to chemical repellents." EMBO J **24**(1): 63-72.

Hu, Z., D. S. Sankar, B. Vu, A. Leytens, C. Vionnet, W. Wu, M. Stumpe, E. Martínez-Martínez, B. Stork and J. Dengjel (2021). "ULK1 phosphorylation of striatin activates protein phosphatase 2A and autophagy." Cell Rep **36**(13): 109762.

Huang, Y., S.-R. Chen, H. Chen, Y. Luo and H.-L. Pan (2020). "Calcineurin Inhibition Causes α2δ-1–Mediated Tonic Activation of Synaptic NMDA Receptors and Pain Hypersensitivity." **40**(19): 3707-3719.

Huang, Y., S.-R. Chen and H.-L. Pan (2022). "Calcineurin Regulates Synaptic Plasticity and Nociceptive Transmission at the Spinal Cord Level." **28**(6): 628-638.

Isensee, J., M. Diskar, S. Waldherr, R. Buschow, J. Hasenauer, A. Prinz, F. Allgöwer, F. W. Herberg and T. Hucho (2014). "Pain modulators regulate the dynamics of PKA-RII phosphorylation in subgroups of sensory neurons." Journal of Cell Science **127**(1): 216-229.

Johnson, J. L., T. M. Yaron, E. M. Huntsman, A. Kerelsky, J. Song, A. Regev, T.-Y. Lin, K. Liberatore, D. M. Cizin, B. M. Cohen, N. Vasan, Y. Ma, K. Krismer, J. T. Robles, B. van de Kooij, A. E. van Vlimmeren, N. Andrée-Busch, N. F. Käufer, M. V. Dorovkov, A. G. Ryazanov, Y. Takagi, E. R. Kastenhuber, M. D. Goncalves, B. D. Hopkins, O. Elemento, D. J. Taatjes, A. Maucuer, A. Yamashita, A. Degterev, M. Uduman, J. Lu, S. D. Landry, B. Zhang, I. Cossentino, R. Linding, J. Blenis, P. V. Hornbeck, B. E. Turk, M. B. Yaffe and L. C. Cantley (2023). "An atlas of substrate specificities for the human serine/threonine kinome." Nature **613**(7945): 759-766.

Jordan, A. and D. A. Glauser (2023). "Distinct clusters of human pain gene orthologs in Caenorhabditis elegans regulate thermo-nociceptive sensitivity and plasticity." Genetics **224**(1).

Kaplan, J. M. and H. R. Horvitz (1993). "A dual mechanosensory and chemosensory neuron in Caenorhabditis elegans." Proc Natl Acad Sci U S A **90**(6): 2227-2231.

Ke, C., Y. Huang, Z. Mao, Z. Ke, Z. Wang, R. Li, S. Long, Y. Guo, F. Wang, M. Qian, R. Zhao, J. Zheng and S. Xie (2023). "Calcineurin suppresses rat H9c2 cardiomyocyteprotective autophagy under chronic intermittent hypoxia by downregulating the AMPK pathway." Exp Cell Res **433**(2): 113850.

Kidd, B. L. and L. A. Urban (2001). "Mechanisms of inflammatory pain." BJA: British Journal of Anaesthesia **87**(1): 3-11.

Kimura, K. D., A. Miyawaki, K. Matsumoto and I. Mori (2004). "The C. elegans Thermosensory Neuron AFD Responds to Warming." Current Biology **14**(14): 1291-1295.

Kimura, Y., E. E. Corcoran, K. Eto, K. Gengyo-Ando, M.-a. Muramatsu, R. Kobayashi, J. H. Freedman, S. Mitani, M. Hagiwara, A. R. Means and H. Tokumitsu (2002). "A CaMK cascade activates CRE-mediated transcription in neurons of Caenorhabditis elegans." EMBO Rep **3**(10): 962-966.

Klee, C. B., T. H. Crouch and M. H. Krinks (1979). "Calcineurin: a calcium- and calmodulin-binding protein of the nervous system." Proc Natl Acad Sci U S A **76**(12): 6270-6273.

Kotera, I., N. A. Tran, D. Fu, J. H. Kim, J. Byrne Rodgers and W. S. Ryu (2016). "Pan-neuronal screening in Caenorhabditis elegans reveals asymmetric dynamics of AWC neurons is critical for thermal avoidance behavior." eLife **5**: e19021.

Kuhara, A., H. Inada, I. Katsura and I. Mori (2002). "Negative Regulation and Gain Control of Sensory Neurons by the C. elegans Calcineurin TAX-6." Neuron **33**(5): 751-763.

Kuner, R. and H. Flor (2017). "Structural plasticity and reorganisation in chronic pain." Nature Reviews Neuroscience **18**(1): 20-30.

Lee, J., C. Jee, H. O. Song, J. Bandyopadhyay, J. I. Lee, J. R. Yu, J. Lee, B. J. Park and J. Ahnn (2004). "Opposing functions of calcineurin and CaMKII regulate G-protein signaling in egg-laying behavior of C.elegans." J Mol Biol **344**(2): 585-595.

Lee, J., H. O. Song, C. Jee, L. Vanoaica and J. Ahnn (2005). "Calcineurin regulates enteric muscle contraction through EXP-1, excitatory GABA-gated channel, in C. elegans." J Mol Biol **352**(2): 313-318.

Lee, J. C., Y. G. Kwon, D. S. Lawrence and A. M. Edelman (1994). "A requirement of hydrophobic and basic amino acid residues for substrate recognition by Ca2+/calmodulin-dependent protein kinase Ia." Proc Natl Acad Sci U S A **91**(14): 6413-6417.

Lemieux, George A., Katherine A. Cunningham, L. Lin, F. Mayer, Z. Werb and K. Ashrafi (2015). "Kynurenic Acid Is a Nutritional Cue that Enables Behavioral Plasticity." Cell **160**(1): 119-131.

Li, W., L. Kang, B. J. Piggott, Z. Feng and X. Z. S. Xu (2011). "The neural circuits and sensory channels mediating harsh touch sensation in Caenorhabditis elegans." Nat Commun **2**: 315.

Li, Z., J. Zhou, K. A. Wani, T. Yu, E. A. Ronan, B. J. Piggott, J. Liu and X. Z. S. Xu (2023). "A C. elegans neuron both promotes and suppresses motor behavior to fine tune motor output." **16**.

Lia, A.-S. and D. A. Glauser (2020). "A system for the high-throughput analysis of acute thermal avoidance and adaptation in C. elegans." J Biol Methods.

Liang, R. J., X. L. Liu, L. M. Wei, W. Wang, P. Zheng, X. S. Yan, Y. L. Zhao, L. J. Liu and X. H. Cao (2012). "The modulation of the excitability of primary sensory neurons by Ca2+-CaM-CaMKII pathway." Neurological Sciences **33**(5): 1083-1093.

Lim, J. P., H. Fehlauer, A. Das, G. Saro, D. A. Glauser, A. Brunet and M. B. Goodman (2018). "Loss of CaMKI Function Disrupts Salt Aversive Learning in C. elegans." J Neurosci **38**(27): 6114-6129.

Liu, J., J. D. Farmer, Jr., W. S. Lane, J. Friedman, I. Weissman and S. L. Schreiber (1991). "Calcineurin is a common target of cyclophilin-cyclosporin A and FKBP-FK506 complexes." Cell **66**(4): 807-815.

Liu, S., E. Schulze and R. Baumeister (2012). "Temperature- and Touch-Sensitive Neurons Couple CNG and TRPV Channel Activities to Control Heat Avoidance in Caenorhabditis elegans." PLoS One **7**(3): e32360.

May, A., R. Rodriguez-Raecke, A. Schulte, K. Ihle, M. Breimhorst, F. Birklein and T. P. Jürgens (2012). "Within-session sensitization and between-session habituation: A robust physiological response to repetitive painful heat stimulation." European Journal of Pain **16**(3): 401-409.

Molkentin, J. D. (2004). "Calcineurin-NFAT signaling regulates the cardiac hypertrophic response in coordination with the MAPKs." Cardiovasc Res **63**(3): 467-475.

Moss, B. J., L. Park, C. L. Dahlberg and P. Juo (2016). "The CaM Kinase CMK-1 Mediates a Negative Feedback Mechanism Coupling the C. elegans Glutamate Receptor GLR-1 with Its Own Transcription." PLoS Genet **12**(7): e1006180.

Mukherjee, A. and C. Soto (2011). "Role of calcineurin in neurodegeneration produced by misfolded proteins and endoplasmic reticulum stress." Curr Opin Cell Biol **23**(2): 223-230.

Neal, S. J., A. Takeishi, M. P. O'Donnell, J. Park, M. Hong, R. A. Butcher, K. Kim and P. Sengupta (2015). "Feeding state-dependent regulation of developmental plasticity via CaMKI and neuroendocrine signaling." eLife **4**: e10110.

Nkambeu, B., J. B. Salem and F. Beaudry (2020). "Capsaicin and Its Analogues Impede Nocifensive Response of Caenorhabditis elegans to Noxious Heat." Neurochem Res **45**(8): 1851-1859.

O'Neill, J., C. Brock, A. E. Olesen, T. Andresen, M. Nilsson and A. H. Dickenson (2012). "Unravelling the mystery of capsaicin: a tool to understand and treat pain." Pharmacological reviews **64**(4): 939-971.

Pace, M. C., M. B. Passavanti, L. De Nardis, F. Bosco, P. Sansone, V. Pota, M. Barbarisi, A. Palagiano, F. A. Iannotti, E. Panza and C. Aurilio (2018). "Nociceptor plasticity: A closer look." Journal of Cellular Physiology **233**(4): 2824-2838.

Perez-Riverol, Y., J. Bai, C. Bandla, D. García-Seisdedos, S. Hewapathirana, S. Kamatchinathan, D. J. Kundu, A. Prakash, A. Frericks-Zipper, M. Eisenacher, M. Walzer, S. Wang, A. Brazma and J. A. Vizcaíno (2022). "The PRIDE database resources in 2022: a hub for mass spectrometry-based proteomics evidences." Nucleic Acids Res **50**(D1): D543-d552.

Peuker, K., A. Strigli, D. V. F. Tauriello, A. Hendricks, W. von Schönfels, G. Burmeister, M. Brosch, A. Herrmann, S. Krüger, J. Nitsche, L. Južnić, M. M. Geissler, A. Hiergeist, A. Gessner, J. Wirbel, R. P. Ponnudurai, A. Tunger, R. Wehner, D. E. Stange, J. Weitz, D. E. Aust, G. B. Baretton, M. Schmitz, C. Röcken, J. Hampe, S. Hinz, G. Zeller, T. Chavakis, C. Schafmayer, E. Batlle and S. Zeissig (2022). "Microbiota-dependent activation of the myeloid calcineurin-NFAT pathway inhibits B7H3- and B7H4-dependent anti-tumor immunity in colorectal cancer." Immunity **55**(4): 701-717.e707.

Piggott, B. J., J. Liu, Z. Feng, S. A. Wescott and X. Z. Xu (2011). "The neural circuits and synaptic mechanisms underlying motor initiation in C. elegans." Cell **147**(4): 922-933.

Rodriguez-Raecke, R., B. Doganci, M. Breimhorst, A. Stankewitz, C. Buchel, F. Birklein and A. May (2010). "Insular cortex activity is associated with effects of negative expectation on nociceptive long-term habituation." J Neurosci **30**(34): 11363-11368.

Rusnak, F. and P. Mertz (2000). "Calcineurin: form and function." Physiol Rev **80**(4): 1483-1521.

Sandkühler, J. (2009). "Models and Mechanisms of Hyperalgesia and Allodynia." Physiological Reviews **89**(2): 707-758.

Saro, G., A. S. Lia, S. Thapliyal, F. Marques, K. E. Busch and D. A. Glauser (2020). "Specific Ion Channels Control Sensory Gain, Sensitivity, and Kinetics in a Tonic Thermonociceptor." Cell Rep **30**(2): 397-408 e394.

Sato, Y., T. Onaka, E. Kobayashi and N. Seo (2007). "The differential effect of cyclosporine on hypnotic response and pain reaction in mice." Anesth Analg **105**(5): 1489-1493, table of contents.

Satterlee, J. S., W. S. Ryu and P. Sengupta (2004). "The CMK-1 CaMKI and the TAX-4 Cyclic nucleotide-gated channel regulate thermosensory neuron gene expression and function in C. elegans." Curr Biol **14**(1): 62-68.

Schild, Lisa C., L. Zbinden, Harold W. Bell, Yanxun V. Yu, P. Sengupta, Miriam B. Goodman and Dominique A. Glauser (2014). "The Balance between Cytoplasmic and Nuclear CaM Kinase-1 Signaling Controls the Operating Range of Noxious Heat Avoidance." Neuron **84**(5): 983-996.

Shum, F. W. F., S. W. Ko, Y.-S. Lee, B.-K. Kaang and M. Zhuo (2005). "Genetic alteration of anxiety and stress-like behavior in mice lacking CaMKIV." Molecular Pain **1**(1): 22.

Smith, B. W., E. M. Tooley, E. Q. Montague, A. E. Robinson, C. J. Cosper and P. G. Mullins (2008). "Habituation and sensitization to heat and cold pain in women with fibromyalgia and healthy controls." PAIN **140**(3): 420-428.

Smith, H. S. (2009). "Calcineurin as a nociceptor modulator." Pain Physician **12**(4): E309-318.

Swierczek, N. A., A. C. Giles, C. H. Rankin and R. A. Kerr (2011). "High-throughput behavioral analysis in C. elegans." Nat Methods **8**(7): 592-598.

Thapliyal, S., I. Beets and D. A. Glauser (2023). "Multisite regulation integrates multimodal context in sensory circuits to control persistent behavioral states in C. elegans." Nature Communications **14**(1): 3052.

Treede, R. D. (1995). "Peripheral acute pain mechanisms." Ann Med **27**(2): 213-216.

Tyanova, S., T. Temu, P. Sinitcyn, A. Carlson, M. Y. Hein, T. Geiger, M. Mann and J. Cox (2016). "The Perseus computational platform for comprehensive analysis of (prote)omics data." Nat Methods **13**(9): 731-740.

Wang, H., Y. Du, B. Xiang, W. Lin, X. Li and Q. Wei (2008). "A renewed model of CNA regulation involving its C-terminal regulatory domain and CaM." Biochemistry **47**(15): 4461-4468.

Wang, H. and M. Zhang (2012). The role of Ca2+-stimulated adenylyl cyclases in bidirectional synaptic plasticity and brain function. Reviews in the Neurosciences. **23:** 67.

White, R. R., Y. G. Kwon, M. Taing, D. S. Lawrence and A. M. Edelman (1998). "Definition of optimal substrate recognition motifs of Ca2+-calmodulin-dependent protein kinases IV and II reveals shared and distinctive features." J Biol Chem **273**(6): 3166-3172.

Willis Jr., W. D. (2001). "Role of Neurotransmitters in Sensitization of Pain Responses." Annals of the New York Academy of Sciences **933**(1): 142-156.

Wittenburg, N. and R. Baumeister (1999). "Thermal avoidance in Caenorhabditis elegans: an approach to the study of nociception." Proc Natl Acad Sci U S A **96**(18): 10477-10482.

Yu, Y. V., H. W. Bell, D. Glauser, S. D. Van Hooser, M. B. Goodman and P. Sengupta (2014). "CaMKI-dependent regulation of sensory gene expression mediates experience-dependent plasticity in the operating range of a thermosensory neuron." Neuron **84**(5): 919-926.

Yuan, Y. P., Z. Y. Shen, T. Teng, S. C. Xu, C. Y. Kong, X. F. Zeng, A. H. B. M and L. Yan (2024). "S100a8/9 (S100 Calcium Binding Protein a8/9) Promotes Cardiac Hypertrophy Via Upregulation of FGF23 (Fibroblast Growth Factor 23) in Mice." J Am Heart Assoc **13**(10): e028006.

Zhou, Y.-Q., D.-Q. Liu, S.-P. Chen, J. Sun, X.-R. Zhou, F. Luo, Y.-K. Tian and D.-W. Ye (2017). "Cellular and Molecular Mechanisms of Calcium/Calmodulin-Dependent Protein Kinase II in Chronic Pain." Journal of Pharmacology and Experimental Therapeutics **363**(2): 176.

865 **FIGURES AND LEGENDS**

866

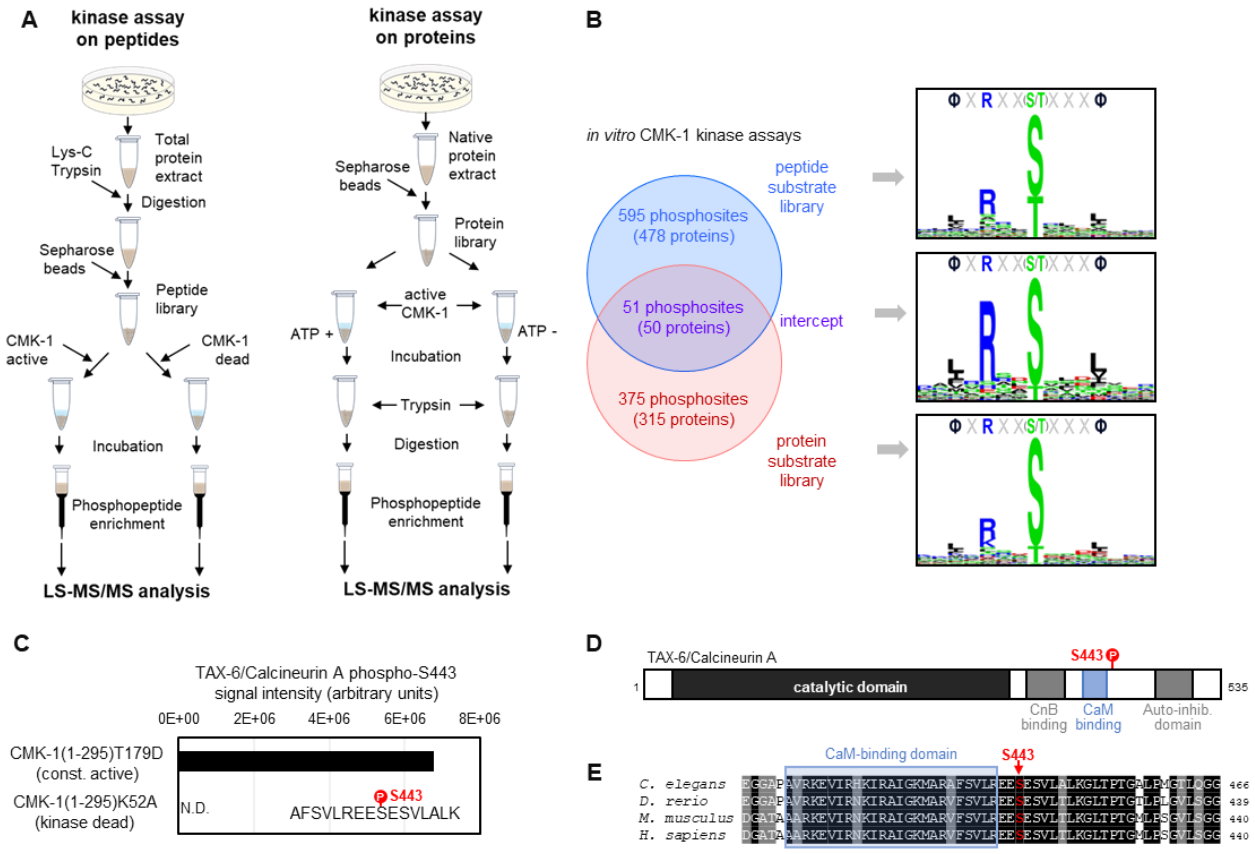

867

868 **Figure 1 Identification of CMK-1 phosphorylation substrates**

869 **A**. Schematic of the two approaches used for the large-scale identification of the CMK-1
870 phosphorlyation substrates *in vitro*. *In vitro* kinase assays using a *C. elegans* peptide library (left)
871 or a *C. elegans* native protein library (right) were followed by MS-based phosphoproteomics
872 analyses. The activity of a constitutively active mutant (CMK-1(1-295)T179D) was compared to
873 control situations with either kinase dead mutant (CMK-1(1-295)K52A) or without ATP co-
874 substrate during the incubation. **B**. Comparison of the results with the two approaches, showing
875 the number of overlapping and non-overlapping phosphosites, the number of corresponding
876 proteins, as well as the 15-residue consensus sequence surrounding the phosphosites. Logos
877 created with Seq2Logo. **C**. Results of a separate *in vitro* kinase assay in which purified TAX-
878 6/CnA was used as substrate and showing TAX-6/CnA S443 phosphorylation. N.D., not detected
879 **D**. Diagram presenting the different regions of the *C. elegans* TAX6/CnA protein and the
880 localization of S443. **E**. Alignments showing high conservation of a CnA protein region around
881 S443 across *C. elegans, Danio rerio, Mus Musculus* and *Homo sapiens* (Uniprot assessions:
882 Q0G819-2|PP2B_CAEEL; A3KGZ6|A3KGZ6_DANRE; P63328|PP2BA_MOUSE;
883 Q08209|PP2BA_HUMAN).

884

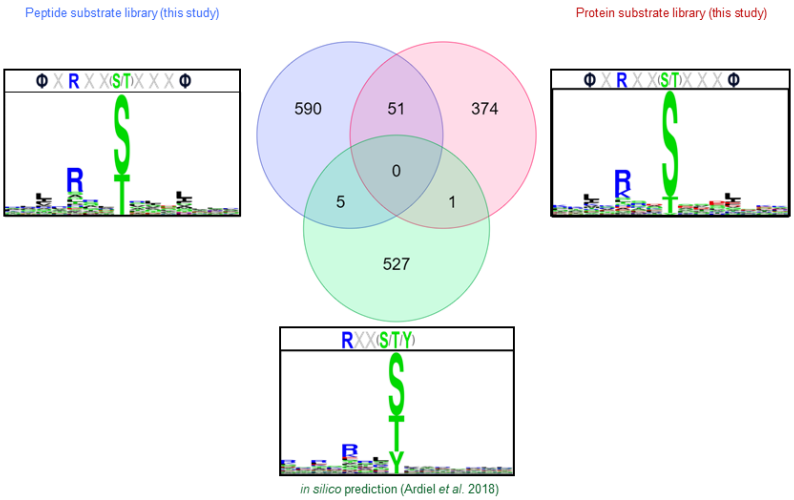

885

886 **Figure 1 -supplement 1 Comparison of empirically identified CMK-1 phospho-substrates**
887 **with previously published predictions**

888 Venn diagram showing the number of phosphosites from the indicated lists and the consensus
889 as in Fig. 1.

890

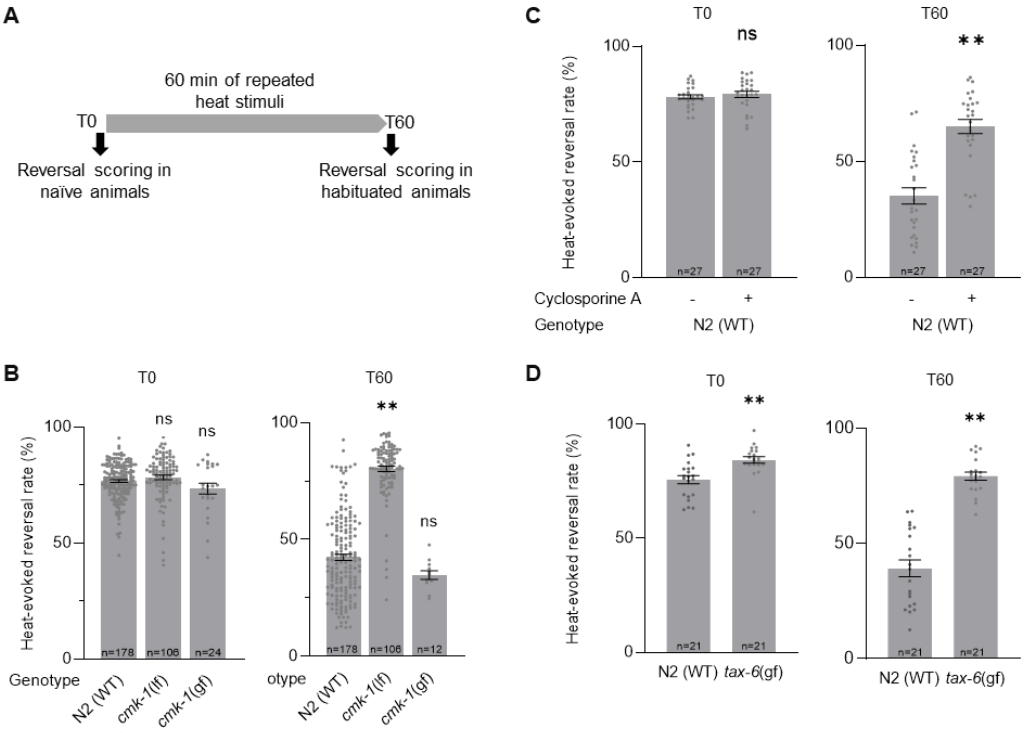

Figure 2 Impact of loss and gain of CMK-1 and TAX-6/CnA function on *C. elegans* thermo-nociceptive response

A. Schematic of the scoring procedure. Heat-evoked reversals were first scored in naïve adult *C. elegans* that had never been exposed to thermal stimuli (T0), animals exposed to 4 s heat pulses every 20 s during 60 min, prior to an endpoint scoring after habituation (T60). **B-D**. Heat-evoked reversal scored in the indicated genotypes. Results as fraction of reversing animals. Each point corresponds to one assay scoring at least 50 animals. Average (grey bars) and s.e.m (error bars) with indicated *n* representing the number of independent assays. *cmk-1(gf)* is *cmk-1(syb1633)*. *cmk-1(lf)* is *cmk-1(ok287)*. *tax-6(gf)* is *tax-(j107)*. For Calcineurin inhibition, 10 µM Cyclosporin A was used 24 prior to experiments. **, $p<.01$ and *, $p<.05$ versus N2(WT) control in the specific condition by Bonferroni-Holm post-hocs tests. ns, not significant.

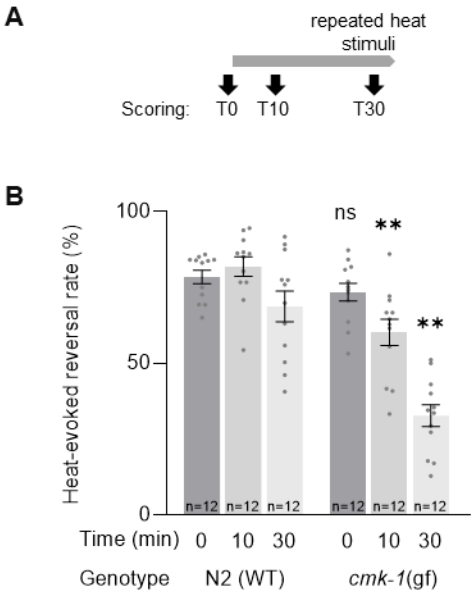

Figure 2-supplement 1 CMK-1 overactivating mutation T179D accelerates thermo-nociceptive habituation

A. Schematic of the scoring procedure variation, including earlier scoring timepoints after 10 and 30 min of repeated noxious heat stimuli. **B**. Heat-evoked reversal scored in the indicated genotypes and reported as in Fig. 2. *cmk-1(gf)* is *cmk-1(syb1633)* harboring the CMK-1(T179D) overactivating mutation. *, $p<.01$ versus corresponding timepoint in N2(WT) control.

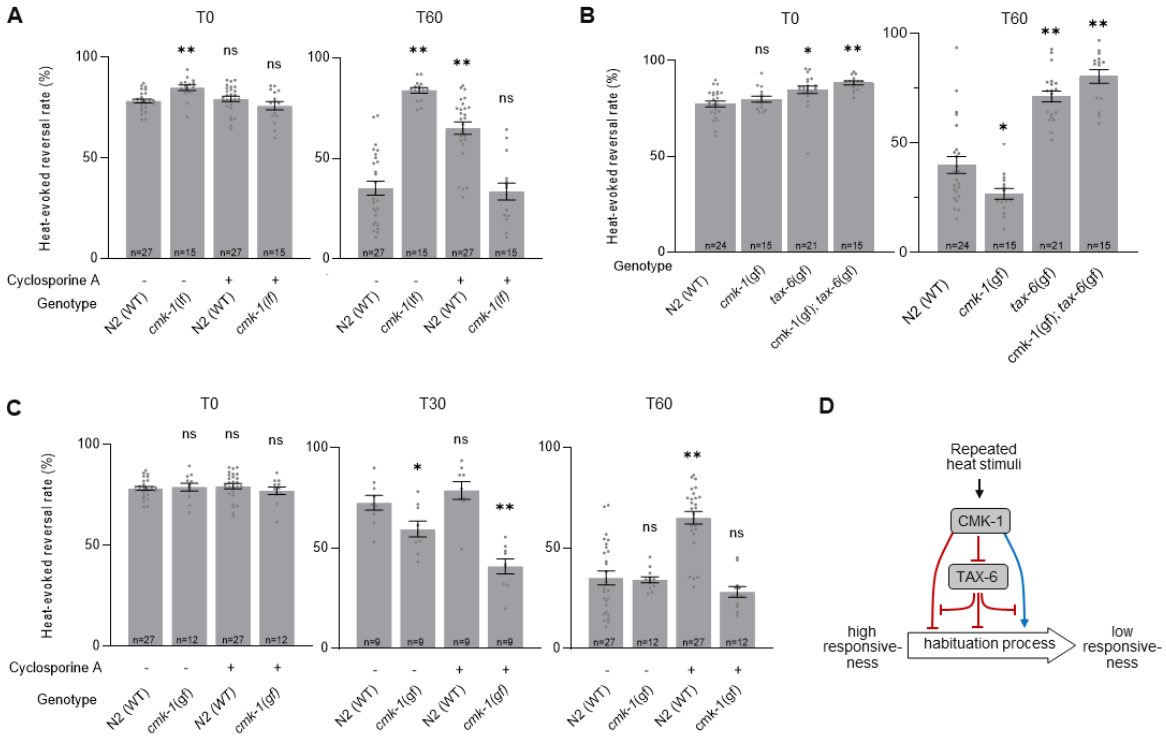

Figure 3 Functional interactions between CMK-1 and TAX-6/CnA in the regulation of thermo-nociceptive habituation

A-C. Assessment of the impact of joint gain- and loss-of-function manipulations affecting the CMK-1 and TAX-6/CnA pathways. Heat-evoked response in naïve animals (T0) and after 60 min of repeated stimulations (T60), scored and reported as in Fig. 2. **, $p<.01$ and *, $p<.05$ versus N2(WT) control in the specific condition by Bonferroni-Holm post-hocs tests. ns, not significant. **D**. Schematic of a model explaining the multiple antagonistic interactions observed between CMK-1 and TAX-6/CnA signaling.

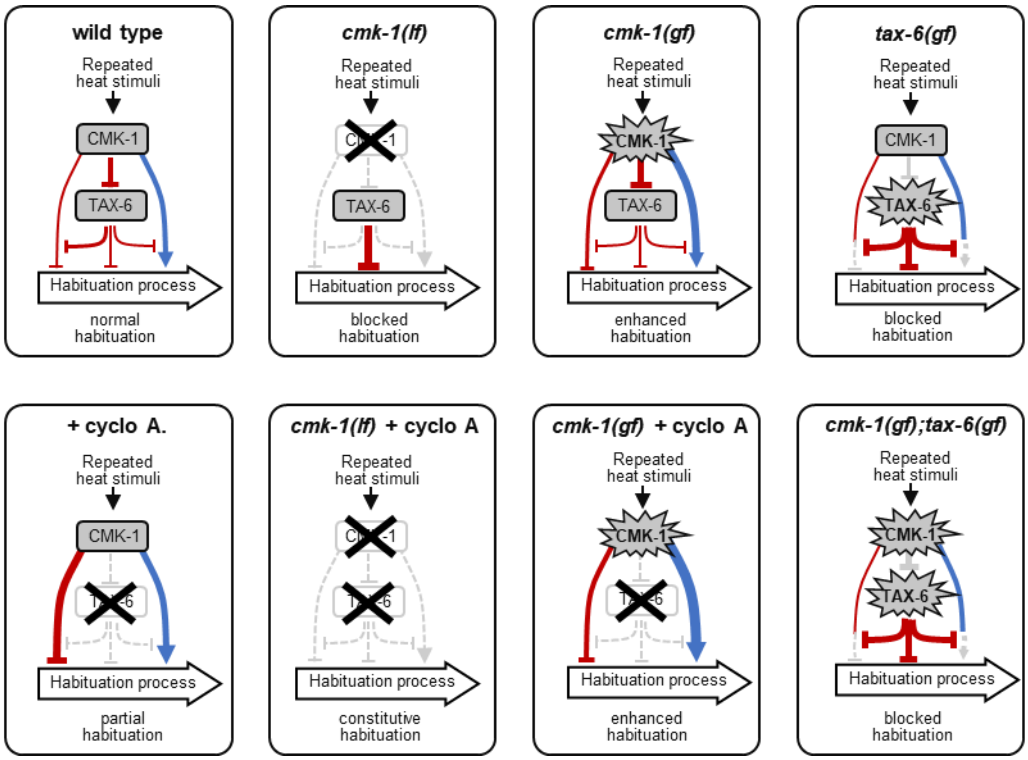

Figure 3- supplement 1 Model of the multiple antagonistic interactions observed between CMK-1 and TAX-6/CnA signaling. Illustration of how the model from Fig. 3D is proposed to be altered for each of the single or combined gain- and loss-of-function manipulations used in Fig. 3. We do not rule out that alternative models might also explain our data, but the model presented in Fig. 3D is the simplest that could explain the complex set of interactions.

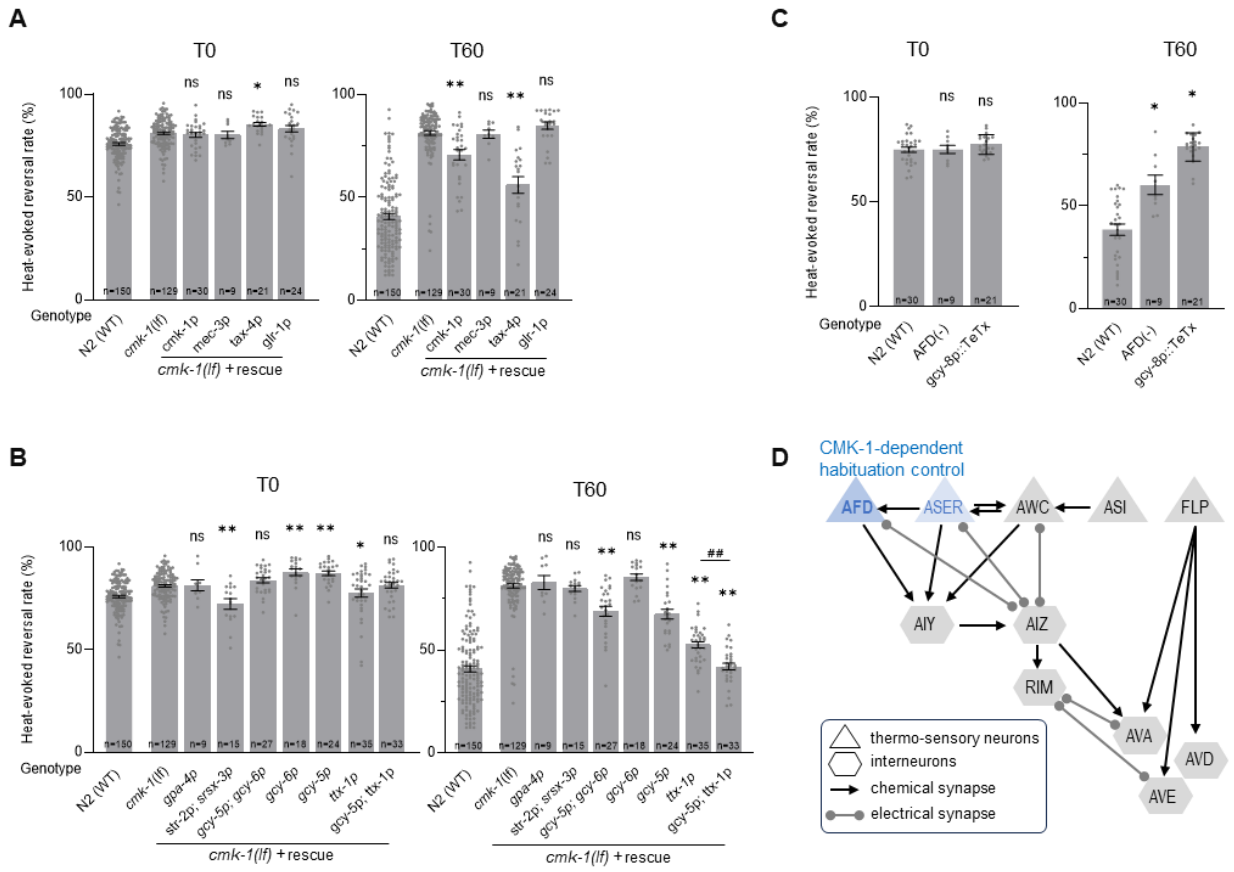

Figure 4. CMK-1 works in AFD and ASER to control thermo-nociceptive habituation

A-B. Determination of the CMK-1 place of action in the control of thermo-nociceptive habituation, using cell-specific rescue in *cmk-1(ok287)* (*cmk-1(lf)*) background. Heat-evoked response in naïve animals (T0) and after 60 min of repeated stimulations (T60), scored and reported as in Fig. 2. The promoters used to restore CMK-1 expression are indicated below each bar. **, $p<.01$ and *, $p<.05$ versus *cmk-1(lf)* by Bonferroni-Holm post-hocs tests. ns, not significant. ##, $p<.01$ for the specific contrast between *ttx-1p* and the *gcy-5p;ttx-1p* combination. N2(WT) data are shown for comparison purpose. **C**. Impact of genetic manipulation ablating AFD with a caspase construct (AFD(-)) or inhibiting AFD neurotransmission with TeTx heterologous expression. **, $p<.01$ and *, $p<.05$ versus N2(WT) control by Bonferroni-Holm post-hocs tests **D**. Schematic of the hypothetical circuit controlling noxious-heat evoked reversals, including the *tax-4*-expressing thermo-responsive sensory neurons AFD, AWC, ASER and ASI, the *mec-3*-expressing FLP thermo-nociceptor, and a subset of downstream interneurons known to mediate reversal response, including the *glr-1*-expressing RIM, AVA, AVD, and AVE interneurons. The main loci of action of CMK-1 determined through the cell-specific rescue approach are highlighted in blue.

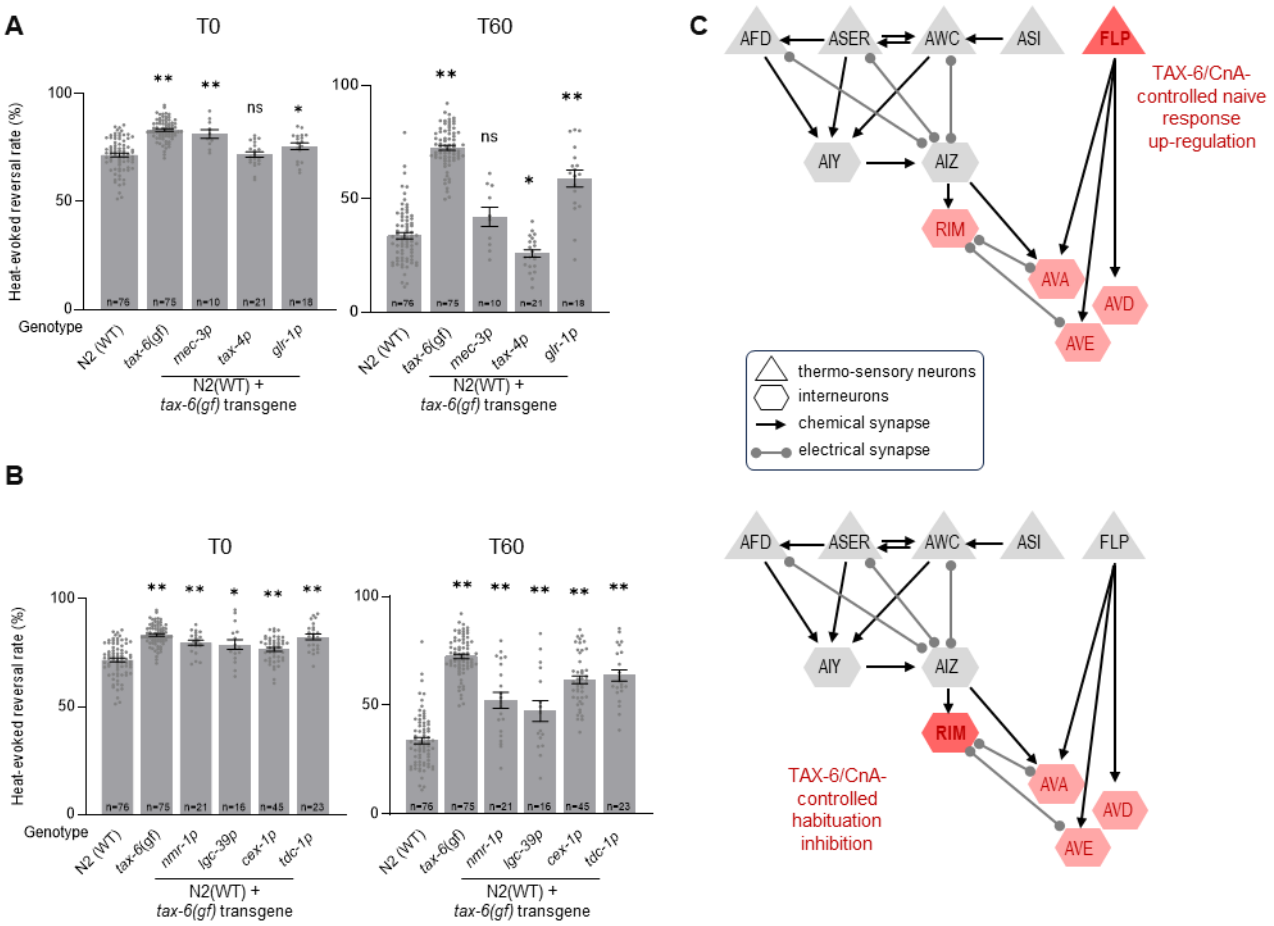

Figure 5. TAX-6/CnA activity in RIM and AVA/AVD/AVE inhibit thermo-nociceptive habituation

A-B. Determination of the TAX-6/CnA place of action in the control of thermo-nociceptive responses, using cell-specific expression of a TAX-6/CnA gain-of-function mutant. Heat-evoked response in naïve animals (T0) and after 60 min of repeated stimulations (T60), scored and reported as in Fig. 2. The promoters used to drive *tax-6(gf)* cDNA expression are indicated below each bar. **, $p<.01$ and *, $p<.05$ versus N2(WT) by Bonferroni-Holm post-hocs tests. ns, not significant. *tax-6(gf)* mutant data are shown for comparison purpose. **C**. Schematics of the hypothetical circuit controlling noxious-heat evoked reversals as in Fig. 4D, with the main loci of action of TAX-6/CnA highlighted in red. TAX-6/CnA-evoked up-regulation of thermo-nociceptive response in naïve animals (top) and TAX-6/CnA-evoked inhibition of habituation (bottom).